



Published in final edited form as:

Toxicol In Vitro. 2015 February ; 29(1): 195–203. doi:10.1016/j.tiv.2014.10.008.

Influence of Physicochemical Properties of Silver Nanoparticles on Mast Cell Activation and Degranulation

Abdullah A. Aldossari^{a,*}, Jonathan H. Shannahan^{a,*}, Ramakrishna Podila^{b,c}, and Jared M. Brown^a

^aDepartment of Pharmaceutical Sciences, Skaggs School of Pharmacy and Pharmaceutical Sciences, The University of Colorado Anschutz Medical Campus, Aurora, Colorado, 80045, USA

^bDepartment of Physics and Astronomy, Clemson University, Clemson, South Carolina, 29634, USA

^cClemson Nanomaterials Center and COMSET, Clemson University, Anderson, South Carolina, 29625, USA

Abstract

Silver nanoparticles (AgNPs) are increasingly being incorporated into products for their antimicrobial properties. This has resulted in increased human exposures and the possibility of adverse health effects. Mast cells orchestrate allergic immune responses through degranulation and release of pre-formed mediators. Little data exists on understanding interactions of AgNPs with mast cells and the properties that influence activation and degranulation. Using bone marrow-derived mast cells and AgNPs of varying physicochemical properties we tested the hypothesis that AgNP physicochemical properties influence mast cell degranulation and osteopontin production. AgNPs evaluated included spherical 20 nm and 110 nm suspended in either polyvinylpyrrolidone (PVP) or citrate, Ag plates suspended in PVP of diameters between 40–60 nm or 100–130 nm, and Ag nanowires suspended in PVP with thicknesses <100 nm and length up to 2 microns. Mast cell responses were found to be dependent on the physicochemical properties of the AgNP. Further, we determined a role for scavenger receptor B1 in AgNP-induced mast cell responses. Mast cell degranulation was not dependent on AgNP dissolution but was prevented by tyrosine kinase inhibitor pretreatment. This study suggests that exposure to AgNPs may elicit adverse mast cell responses that could contribute to the initiation or exacerbation of allergic disease.

© 2014 Elsevier Ltd. All rights reserved.

Corresponding author: Jared M. Brown, Ph.D., Department of Pharmaceutical Sciences, Skaggs School of Pharmacy and Pharmaceutical Sciences, The University of Colorado Anschutz Medical Campus, 12850 E. Montview Blvd, Mail Stop C238, Aurora, CO 80045, jared.brown@ucdenver.edu, 303-724-8213.

* Authors contributed equally to the manuscript.

Publisher's Disclaimer: This is a PDF file of an unedited manuscript that has been accepted for publication. As a service to our customers we are providing this early version of the manuscript. The manuscript will undergo copyediting, typesetting, and review of the resulting proof before it is published in its final citable form. Please note that during the production process errors may be discovered which could affect the content, and all legal disclaimers that apply to the journal pertain.

Keywords

Silver nanoparticles; bone marrow-derived mast cell; Scavenger Receptor B1; Lamp2; Osteopontin

Introduction

The applications of nanotechnology are rapidly expanding and revolutionizing many fields primarily through the incorporation of nanoparticles (NPs) into numerous biomedical and consumer products. In particular, silver nanoparticles (AgNPs) are one of the most utilized NPs due to their antimicrobial/fungal properties (Dong et al., 2012; Levard et al., 2013; Nocchetti et al., 2013). More than 300 globally available consumer products, such as wound dressings, IV bags, dermal creams, water filters, and many household products, incorporate AgNPs (Project, 2014). Indeed, the annual global production of AgNPs is estimated to be >55 tons (Piccinno et al., 2012). A direct interaction of end user and AgNP-based products increases the risk of possible exposure through Ag or Ag⁺ leaching out from these products and could possibly result in adverse health outcomes (Christensen et al., 2010). For instance, AgNPs used as coatings on surgical implants may enter into the systemic circulation and translocate into different organs such as the lung and/or liver (Rahman et al., 2009; Tang et al., 2009). More importantly, some food storage containers that use AgNP coatings that have been found to release nanostructured Ag into food due to an increase dissolution under high salt concentration (Echegoyen and Nerín, 2013). Animal studies have demonstrated that AgNP exposure results in hepatotoxicity and pulmonary inflammation (Sung et al., 2008; Tiwari et al., 2011). In addition, AgNPs have been reported to interact with immune cells and induce cytotoxicity through the generation of reactive oxygen species (Carlson et al., 2008; Nishanth et al., 2011). To date, limited research exists evaluating the ability of NPs to directly interact with immune cells involved in allergy such as mast cells and possibly resulting in or exacerbation of allergic disease.

Mast cells are found in most tissue types and play an important role in innate immunity, host defense and allergic disease (Brown et al., 2008). Mast cells are well studied for their role in allergic disease and activation through IgE and the high affinity IgE receptor (FcεRI) leading to the release of a variety of mediators including histamine, serotonin, and inflammatory cytokines such as TNF-α, osteopontin (OPN), and eosinophil chemoattractant factor as examples (Brown et al., 2008). In addition, mast cells recognize pathogens through toll-like receptors and scavenger receptors (McCurdy et al., 2003; Medic et al., 2008). Recent animal studies have demonstrated that mast cells contribute to the inflammatory response following NP exposures. Specifically, it has been reported that mast cells are involved in lung inflammation and fibrosis following exposure to multi-walled carbon nanotubes (MWCNTs) (Katwa et al., 2012). In addition, mast cells have been shown to be involved in cerium oxide-induced alterations in vascular reactivity (Wingard et al., 2011). Even though mast cells appear to be central in the pathogenesis following NP exposure little research has been done assessing the direct interaction of NPs with mast cells. While mast cells are well-known to be involved in allergic conditions, it is currently unclear if NPs have the capacity to induce and/or promote an allergic disease state (Podila and Brown, 2013;

Shannahan and Brown, 2014; Shannahan et al., 2012). One study reported that AgNPs can induce mast degranulation in the RBL-2H3 rat basophilic cell line, however, the study was focused on real-time live cell imaging of the degranulation process but not the influence of physicochemical properties of AgNPs (Yang et al., 2010). In another study, researchers used mouse peritoneal mast cells to compare uptake of spherical Au and Ag NPs (Marquis et al., 2011). This study demonstrated that positively charged NPs were internalized more than negatively charged NPs while mast degranulation was decreased in cells exposed to negatively charged AgNPs.

Scavenger receptors are well known for their role in recognizing and binding lipid molecules such as low-density lipoprotein (LDL) and high-density lipoprotein (HDL) (Goldstein et al., 1979; Krieger and Herz, 1994; Landschulz et al., 1996). Scavenger receptor B1 (SR-B1) is a multi-ligand receptor that preferentially binds lipid molecules and other negatively charged molecules (Krieger and Herz, 1994; Landschulz et al., 1996; Rigotti et al., 1997b). Furthermore, SR-B1 has been reported to recognize and bind with pathogens and NPs (Eyre et al., 2010; Mooberry et al., 2010). Many different types of cells express SR-B1 including epithelial cells, endothelial cells, and macrophages. Specifically, the cellular uptake of AgNPs by macrophages and subsequent apoptosis has been shown to be scavenger receptor dependent (Singh and Ramarao, 2012). Therefore it is likely that other cells, which express scavenger receptors on their surface such as mast cells, may interact with AgNPs similarly and this receptor interaction may mediate toxic responses.

In this study, we hypothesized that NP physicochemical properties such as size, shape, and surface coating will influence mast cell degranulation through interaction with SR-B1. To address this hypothesis, bone marrow derived mast cells were used to assess AgNP directed degranulation using AgNPs of differing size, shape and surface coating. Lastly, we evaluated the role of SR-B1 in the observed mast cell degranulation response to various AgNPs.

Materials and Methods

Silver Nanoparticles

20 and 110 nm spherical AgNPs either suspended in citrate (C20 and C110) or polyvinylpyrrolidone (PVP) (P20 and P110) were procured through the National Centers for Nanotechnology Health Implications (NCNHIR) and initially characterized by the National Characterization Laboratory at the National Cancer Institute. Two types of nanoplates with optical resonance peak at specific wavelengths of 550 nm and 850 nm suspended in PVP (P550 and P850), or Ag nanowires that are up to 2 μ m suspended in PVP were purchased from NanoComposix at a concentration of 1 mg/ml. All AgNPs were negative for endotoxin contamination.

Silver Nanoparticle Characterization

The hydrodynamic size and Zeta potentials (ZetaSizer Nano, Malvern) of all AgNPs were characterized in N-2-hydroxyethylpiperazine-N-2-ethane sulfonic acid (HEPES). All measurements were performed with 3 individual samples at a concentration of 50 μ g/ml.

The size and shape of the AgNPs were confirmed via transmission electron microscopy (TEM, Hitach H7600). Size distribution analysis was performed using the freeware software Image J. A minimum of 100 particles per sample were counted by randomly surveying the entire TEM grid from multiple high magnification images. Image J was used to determine both area and Feret diameters (the greatest distance between two points on an objects boundary).

Reagents and Antibodies

SR-B1 inhibitor 2-(2-butoxyethyl)-1-cyclopentanone thosemicarbazone (Blt2) (Chembridge Corp., San Diego, CA, USA), Rat Lysosome-associated membrane proteins 2 (Lamp2) anti-mouse antibody (eBioscience Inc., San Diego, CA, USA), Imatinib (98%) (Cayman Chemical Company, Ann Arbor, MI, USA)

Cell Culture

Bone marrow-derived mast cells were cultured from femoral marrow cells of C57Bl/6 mice (Jackson Laboratories, Bar Harbor, ME). Bone marrow from 2 mice were used for each batch of mast cells. Cells were cultured in RPMI 1640 medium supplemented with 10% FBS, 100 U/ml penicillin, 100 µg/ml streptomycin, 100 µg/ml Primocin™ (Invivogen, San Diego, CA), 25 mM HEPES, 1.0 mM sodium pyruvate, nonessential amino acids (BioSource International, Camarillo, CA), 0.0035% 2-ME and 300 ng/ml recombinant mouse IL-3 (PeproTech, Rocky Hill, NJ). Mast cells were used following 4–6 weeks of culture at 37°C and 5% CO₂. All animal procedures were conducted in accordance with the National Institutes of Health guidelines and approved by the University of Colorado Denver Institutional Animal Care and Use Committee. All animals were treated humanely and with regard for alleviation of suffering. Cytotoxicity of AgNPs at concentrations used in this study were evaluated by MTS and LDH assays (Promega, Madison WI) and did not induce cytotoxicity compared to the control group (data not shown). Further these concentrations were based on the evaluation of other nanoparticles which have utilized similar concentrations as performed by the NIEHS Nano GO Consortium (Xia et al., 2013).

Enhanced Darkfield Imaging

3×10^5 cells were exposed to AgNPs at concentration of 50 µg/ml for 1 h then washed and spun on a glass slide using a Cytospin IV (Shandon Scientific Ltd., Cheshire, UK) at 300 rpm for 5 min. Cells were then fixed in 2% paraformaldehyde solution for 10 min at 37°C then washed with phosphate-buffered saline (PBS) three times and mounted with DAPI staining ProLong® (Life Technologies, Carlsbad, CA). Cells were then qualitatively assessed by enhanced dark field microscopy (Cytoviva, Auburn, AL) for uptake of AgNPs by focusing on the DAPI stained nucleus.

Inductively Coupled Plasma-Mass Spectrometry (ICP-MS)

3×10^5 cells were pretreated with or without the scavenger receptor B1 (SR-B1) inhibitor Blt2 at a concentration of 50 µM. After 30 min, cells were exposed to AgNPs at concentration of 50 µg/ml for 1 h. Following exposure, samples were collected and centrifuged for 10 min at 14,000 rpm (20,817 g) and washed three times with PBS to

remove excess AgNPs. All samples were dissolved in 6 ml of 2% HNO₃. Subsequently, the Ag cellular concentration was determined with ICP-MS (X series II, Thermo Scientific) using an internal standard containing Li, Y, and In with a resolution of 0.1 ppb. All experiments were performed in triplicate from 3 individual batches of mature mast cells. Each batch of mast cells was grown from femoral bone marrow of 2 mice.

Mast Cell Degranulation

Bone marrow-derived mast cells were seeded at 5×10^4 cells/well in 96-well flat-bottom plates for assessment of degranulation by β -hexosaminidase release (Iwaki et al., 2005). For treated samples, all types of AgNPs were added at 0, 6.25, 12.5, 25, or 50 μ g/ml for 1 h. In addition, 24 h prior to degranulation measurements a subset of cells were sensitized with 100 ng/ml mouse IgE anti-DNP (Sigma-Aldrich, St. Louis, MO) followed by addition of 100 ng/ml dinitrophenylated human serum albumin (DNP-HSA) (Sigma-Aldrich) for 1 h to generate a positive control. For experiments with Blt2, cells were pretreated with Blt2 at 50 μ M for 30 minutes before being exposed to AgNPs. To assess the contribution of ionic Ag to β -hexosaminidase release, AgNPs were placed into HEPES for 1 h, spun at 3000 g for 10 min into Amicon Ultra-15 Centrifugal Filter Units (EMD Millipore). Filtrate containing ionic Ag was used to treat cells. After 1 h incubation of either DNP-HSA or AgNPs at 37°C, *p*-nitrophenyl-*N*-acetyl- β -D-glucopyranoside (98%) was added to cell supernatants and lysates for 90 min as a chromogenic substrate for *N*-acetyl- β -D-hexosaminidase (Sigma-Aldrich) (Brown et al., 2007). The reaction was stopped with 0.4 M glycine. Optical density was measured at 405 nm using a Synergy™ HT Multi-Mode Microplate Reader (BioTek Instruments, Inc, Winooski, VT). β -hexosaminidase release was expressed as the percentage of total cell content after subtracting background release from unstimulated cells. All experiments were performed in triplicate from 3–6 individual batches of mature mast cells. Each batch of mast cells was grown from femoral bone marrow of 2 mice.

Lamp2 Expression

3×10^5 cells were treated with AgNPs, spun at 1200 rpm for 5 min and then suspended in 200 μ l of PBS. Cells were then spun at 300 rpm for 5 min onto a glass slide using a Cytospin IV (Shandon Scientific Ltd., Cheshire, UK). Cells were then fixed in a 2% paraformaldehyde solution for 10 min at 37°C, washed with PBS and blocked in 0.1% Tween + 1% BSA for 30 min at 37°C. After removing blocking solution, a Lamp2 antibody (eBioscience Inc., San Diego, CA, USA) conjugated to FITC was added to slides at a dilution of 1:100 and incubated overnight at 4°C. Following incubation the slide was washed 3 times with PBS and mounted with DAPI staining ProLong® (Life Technologies, Carlsbad, CA). Cells were then assessed using a fluorescent microscope (Cytoviva) to evaluate Lamp2 expression.

Osteopontin Measurement

2.5×10^5 cells were pretreated with or without the scavenger receptor B1 (SR-B1) inhibitor Blt2 at a concentration of 50 μ M. After 30 min, cells were exposed to AgNPs at concentration of 50 μ g/ml for 24 h. OPN levels were measured in cell supernatant using a DuoSet ELISA kit (R&D Systems, Minneapolis, MN) in accordance with the manufacturer's instructions. Values are an average of three replicates and reported as

pg/mL. All experiments were performed in triplicate from 3 individual batches of mature mast cells. Each batch of mast cells was grown from femoral bone marrow of 2 mice.

Statistical Analyses

All data are presented as mean \pm SEM and were analyzed by one-way ANOVA, with differences between groups assessed using Bonferroni post hoc tests. Graphs and analysis were performed using GraphPad Prism 5 software (GraphPad, San Diego, CA). Differences were considered statistically significant at $p < 0.05$.

Results

AgNP Characterization

Hydrodynamic size and zeta potential were measured by dynamic light scattering in HEPES buffer that was used for the subsequent mast cell degranulation studies (Table 1). The hydrodynamic and TEM sizes were similar for the P20, C20, P110, and C110 samples since they are spherical nanoparticles unlike the P550, P850, and wires that have different morphology. It should be noted that the traditional dynamic light scattering technique is based on Einstein-Stokes relation that is apt only for spherical particles and may only provide an order of magnitude estimate for individual dimensions in different direction for non-spherical shapes. In our case, the hydrodynamic size for P550, P850, and wires in HEPES buffer clearly confirms their nanosize while TEM provides more accurate size data. We found that the C20 AgNPs have the smallest hydrodynamic size with an average of 26.61 nm while the Ag nanowires have largest hydrodynamic size with an average of 315 nm ($n=3$ /group). All AgNPs had a negative zeta potential with the citrate suspended AgNPs displaying the most negative surface charge as compared to PVP suspended AgNPs. The shape and size was further confirmed by TEM images of AgNPs (Figure 1).

AgNP Uptake by Mast Cells

Enhanced darkfield imaging of BMMCs following 1 h exposure to AgNPs showed interaction and presence of particles within and on the surface of cells (Figure 2). The surface bound and internalized particles were quantified using ICP-MS analysis ($n=3$ /group) (Figure 3). Following AgNP exposure for 1 h, we found that significant uptake of AgNPs by mast cells occurred in all treated samples. However, pretreatment with the SR-B1 inhibitor significantly decreased the cellular uptake of P20 and P110 (Figure 3).

AgNP Induced Mast Cell Degranulation

Following a 1 h exposure to AgNPs, BMMC degranulation was evaluated through measuring β -hexosaminidase release into the supernatant ($n=3-6$ /group) (Figure 4). P20 and C20 caused significant BMMC degranulation at concentrations of 25 and 50 $\mu\text{g/ml}$ (Figure 4A). P110 and C110 were not found to cause BMMC degranulation compared to control (Figure 4B). P550 and P850 caused significant mast degranulation at all concentrations (Figure 4C). Exposure to Ag nanowires led to an increase in BMMC degranulation at concentrations of 12.5, 25, and 50 $\mu\text{g/ml}$ (Figure 4D). P850 did not demonstrate a concentration-dependent increase in degranulation as shown by P20, C20, and Ag nanowires. To determine whether AgNP or Ag^+ ions were responsible for degranulation,

BMMCs were exposed to Ag⁺ ions for 1 h and degranulation was evaluated. Exposure to Ag⁺ ions was not found to induce mast degranulation (Figure 4E).

To evaluate the role of SR-B1 in degranulation following AgNP exposure, BMMCs were pretreated with or without Blt2 at concentration of 50 μM for 30 min. In this experiment, we evaluated only AgNPs that elicited significant BMMC degranulation (>50%). Following a 1 h exposure to AgNPs at a concentration of 50 μg/ml, β-hexosaminidase was assessed. The degranulation of BMMCs exposed to P20, C20, and Ag nanowires was significantly reduced by pretreatment with the SR-B1 inhibitor Blt2 (Figure 4F).

To confirm our observation of AgNP directed BMMC degranulation measured by β-hexosaminidase release, we assessed lysosome-associated membrane proteins 2 (Lamp2) expression in BMMCs following AgNPs exposure (Figure 5). The expression of Lamp2 following exposure to the various AgNPs was found to match the results of the β-hexosaminidase assay. Lamp2 expression as measured by immunofluorescence (green) was observed in BMMCs exposed to P20, C20, P550, and Ag nanowires while expression of Lamp2 was low in samples treated with P110, C110, and P850 (Figure 5).

Osteopontin Release Following AgNP Exposure

Osteopontin (OPN) levels were measured in the supernatant following exposure to AgNPs (n=3/group) in order to assess AgNP-induced mast cell activation. Mast cells were pretreated with or without Blt2 at concentration of 50 μM for 30 min. Following inhibitor pretreatment, BMMCs were exposed to AgNPs at a concentration of 50 μg/ml for 24 h. OPN levels were increased in the supernatant of BMMCs exposed to all types of AgNPs except for P110 (Figure 6). Pretreatment with Blt2 was found to decrease OPN levels in the supernatant of BMMCs exposed to all types of AgNPs (Figure 6).

Pharmacological Inhibition of Mast Cell Activation by AgNPs

To begin to understand potential mechanisms of AgNP-induced degranulation we pretreated cells with imatinib, a tyrosine kinase inhibitor. BMMCs were pretreated with or without imatinib for 30 min at concentrations of 0.1, 1, 10, and 100 μM and then exposed to C20 at 50 μg/ml for 1 h (n=3/group). Following C20 exposure, β-hexosaminidase release was increased as observed previously, however, treatment with imatinib resulted in a concentration-dependent decrease in BMMC degranulation.

Discussion

Currently we lack sufficient knowledge regarding the ability of these NPs to induce and/or promote allergic disease. Recent studies by our laboratory have demonstrated that mast cells contribute to the inflammation and pathology induced following cerium oxide and carbon-based NP exposure in animal models (Katwa et al., 2012; Wingard et al., 2011). Our current study investigated the direct interactions of physicochemically distinct AgNPs on mast cell activation and degranulation. Further, we evaluated the role of SR-B1 in these AgNP-induced mast cell responses. In summary, this study determined that P20, C20, nanoplates and Ag nanowires could directly induce the degranulation of mast cells. Further this degranulation was driven by particle interactions through the SR-B1 receptor and not the

result of dissolution of Ag⁺ ions. Through evaluation of our data we have provided insight into some of the physicochemical properties of NPs which could likely lead to adverse mast cell responses.

Our study evaluated mast cell responses to AgNPs that differed based upon size, shape, and surface coating. These AgNPs were specifically selected for the determination of NP physicochemical properties, which could influence interactions with mast cells and may initiate or promote allergic responses. Specifically, we selected four spherical AgNPs that differed based on size (20 nm or 110 nm) and surface coating (PVP or Citrate). Further we selected two plate-shaped AgNPs, which differed based upon size and resonance (P550 or P850) and were coated with PVP. Lastly we selected Ag nanowires that differed vastly from the other AgNPs based on their needle-like shape and high aspect ratio. Through the use of these selected AgNPs we were able to determine mast cell responses in terms of specific AgNP characteristics.

The internalization of NPs by mast cells has been reported in different studies. For instance silicon dioxide (SiO₂) and titanium dioxide (TiO₂) was found to be internalized by mast cells and localized in the secretory granules (Maurer-Jones et al., 2010). Following internalization by mast cells, NPs have been reported to induce or suppress mast degranulation. For instance, mast cells have been shown to internalize fullerenes through nonspecific endocytosis causing an inhibition of degranulation (Ryan et al. 2007). In contrast, gold NPs have been reported to induce mast cell degranulation following internalization that was dependent on size, exposure time, and concentration (Huang et al., 2009; Marquis et al., 2009). Overall NP internalization and subcellular localization may play a major role in mast cell activation or suppression, however, limited data are available.

All of our selected AgNPs were found to be internalized following exposure albeit to varying degrees based upon their physicochemical differences. C20 and C110 were determined to have a more highly negative zeta potential compared to PVP suspended spherical AgNPs. However, PVP suspended particles were cell associated to a greater degree when compared to citrate suspended particles of the same size and shape. Such an observation concurs with the fact that PVP stabilized AgNPs are more prone to surface oxidation and subsequently interact strongly with biomolecules (e.g., serum albumin) (Podila et al., 2012). This suggests that uptake of these spherical AgNPs is not completely driven by charge but also the identity of the surface coating. Interestingly P110, P550, and Ag nanowires were found to have similar surface charges (-27.3, -29.6, -25.9 mV respectively) and the same PVP surface coating, however each were internalized at varying amounts. This demonstrates that uptake is also influenced by size and/or shape of the NP. This was not unexpected as the influence of size and shape of NPs has been reported to play critical role in cellular uptake (Miethling-Graff et al., 2014). Lastly, P850 AgNPs were taken up more readily than P550 AgNPs. These plates have the same surface coating, shape but differ based upon size suggesting that size is a major factor in their internalization. Internalization of our selected AgNPs by mast cells is a complex process that seems to be dependent on a combination of physicochemical properties.

The primary objective of this study was to evaluate NP characteristics, which could possibly promote allergic immune responses through direct interaction with mast cells resulting in degranulation and the release of inflammatory mediators. Exposure to spherical 20 nm AgNPs was found to induce mast cell degranulation whereas spherical 110 nm AgNPs did not. Further, exposure to P550 was found to induce degranulation to a greater degree than P850. Even though Ag nanowires and P110 spherical AgNPs existed with a similar surface charge and coating, Ag nanowires were found to induce degranulation whereas the spherical AgNPs did not. NPs with high aspect ratio such as (MWCNTs) have been reported to cause lysosomal damage and induce inflammasome activation that was dependent on NP length (Hamilton et al., 2013; Li et al., 2013). Furthermore, TiO₂ NPs with fiber structure have been found to induce cytotoxicity, reactive oxygen species (ROS) generation, increased expression of inflammatory cytokines, lysosomal damage, and induction of inflammasome activation (Hamilton et al., 2013; Li et al., 2013). While in the present study the Ag nanowires reduced cellular uptake, this shape of AgNPs led to mast cell degranulation likely due to the high aspect ratio of the material (Champion et al., 2007; Champion and Mitragotri, 2006; Harris and Dalhaimer, 2012; Sharma et al., 2010; Sunshine et al., 2014). Overall these findings support a role for size and possibly shape in the degranulation response likely mediated through cell surface receptor recognition.

Similar results have reported that mast cells interact differently with different size and shape of same nanomaterial. For instance, carbon based NPs have been reported to induce mast cell activation as reported with multi-walled carbon nanotubes or can suppress mast cell activation as it has been reported with single-walled carbon nanotubes and fullerene C₆₀ (Huang et al., 2009; Katwa et al., 2012; Ryan et al., 2007; Umemoto et al., 2014). Based on our current findings, mast cell degranulation is not entirely dependent on internalization of the NP. Specifically, both the citrate and PVP suspended spherical 110 nm AgNPs, while internalized by mast cells, were not found to induce degranulation. In comparison, the C20 AgNPs although not internalized to the same degree as the PVP suspended 20 nm AgNPs induce equivalent degranulation. Such an observation is intriguing in that the dissolution of C20 is expected to be much slower than P20 eliminating Ag⁺ as a possible cause for degranulation (Kittler et al., 2010). These findings are consistent with other reports that the uptake of NPs by mast cells causes a variety of mast cell responses including the suppression of mast cell degranulation and decreased reactive oxygen species generation while some have been shown to induce degranulation (Dellinger et al., 2010; Ryan et al., 2007; Umemoto et al., 2014). Our findings suggest cellular signaling initiated by size-dependent NP-cell surface receptor interactions facilitated mast cell degranulation that is not completely driven by NP uptake. Ultimately, through our assessment of physicochemically diverse AgNPs, we have demonstrated that some NPs can directly interact with mast cells inducing degranulation, which could induce and/or promote allergic disease *in vivo*.

Osteopontin is a secreted phosphoglycoprotein expressed by a variety of cell types and has been reported as a risk predictor in various diseases including cardiovascular and cancer such as mesothelioma that associated with asbestos exposure (Berezin and Kremzer, 2013; Pass and Carbone, 2009; Yang et al., 2008). Mast cell activation following NP exposure leads to the release different cytokines such as OPN and has been reported to be up-

regulated following cerium oxide exposure in mice (Wingard et al., 2011). In our current study, we found that OPN is released from mast cells following exposure to all of the selected AgNPs even when NP exposures resulted in limited or no degranulation. These findings are similar to previous research conducted in our laboratory demonstrating that silica exposure also results in cytokine production with limited mast cell degranulation (Brown et al., 2007). This demonstrates that the *de novo* production and release of cytokines from mast cells following particle exposure may involve separate cell signaling pathways compared to degranulation. Our current study also demonstrates that inhibition of the scavenger receptor, SR-B1, reduces the production and release of OPN. Our findings also suggest that while certain NPs do not induce mast cell degranulation, these particles can significantly alter the release of mast cell derived cytokines thereby contributing to an inflammatory response absent of mast cell degranulation. Overall, these findings illustrate that further studies are needed to elucidate mast cell signaling mechanisms.

SR-B1 is well known for its role in the transport of lipid molecules into cells (Krieger and Herz, 1994; Landschulz et al., 1996; Rigotti et al., 1997a). However, it has also been reported that SR-B1 can recognize and bind to other molecules, specifically those that are negatively charged (Baranova et al., 2005; Catanese et al., 2013; Murao et al., 1997). In this study, all AgNPs carried a negative charge therefore interaction between SR-B1 and AgNPs was expected. Inhibition of SR-B1 was found to reduce the uptake of P20, P110, C110, and P850 AgNPs whereas uptake of other AgNPs was unaffected. Due to the range of surface charges exhibited by these AgNPs, SR-B1 recognition and SR-B1 mediated uptake does not appear to be strictly based on NP surface charge. Treatment with an SR-B1 inhibitor (Blt2) was found to reduce mast cell degranulation following exposure to P20, C20, P550, and Ag nanowires. However, SR-B1 inhibition did not reduce degranulation of mast cells induced by P550 AgNPs or Ag nanowires to the same extent as P20 or C20 AgNPs, which were reduced to control levels. Comparatively, P20 and C20 AgNPs have a greater negative Zeta potential and smaller size than P550 and Ag nanowires. These findings suggest that exposure to P20 and C20 AgNPs induces mast cell degranulation through SR-B1 whereas P550 AgNPs and Ag nanowires induce degranulation primarily via other surface receptors or pathways. Overall our use of an SR-B1 inhibitor demonstrates that mast cell responses to AgNP exposure are to some degree mediated through SR-B1. These findings have safety implications for the design of NPs that do not interact with scavenger receptors may reduce the likelihood of unintended allergic responses mediated through mast cells.

Mast cells can be activated through a variety of cell-surface receptor facilitated mechanisms including interactions with SR-B1, FC ϵ RI, or c-Kit. Activation of these receptors leads to increased calcium flux, tyrosine kinase phosphorylation, and ultimately mast cell degranulation (Canton et al., 2013; Zhu et al., 2009) Imatinib is a therapeutic agent that inhibits the phosphorylation of tyrosine kinases thereby inhibiting downstream mast cell degranulation. We determined in this study, that imatinib treatment reduces mast cell degranulation following exposure to C20 AgNPs thereby demonstrating that the NP-induced mast cell degranulation can be therapeutically inhibited. These findings also suggest that there are downstream cell signaling events, which occur following NP cell-surface receptor

interactions that require further investigation. These cellular signaling pathways are likely differentially induced based on NP physicochemical properties and concentrations.

In conclusion this study demonstrates that mast cells can be directly activated by NPs, which may ultimately induce and/or promote an allergic immune response. Further, NP-induced mast cell degranulation is related to the physicochemical properties of the NP such as shape, size, and surface coating. This study implicates a role for SR-B1 in the degranulation of mast cells by NPs and suggests that possible allergic responses to NPs can be therapeutically treated by inhibition of tyrosine kinase phosphorylation. Future research needs to be performed to understand cell-signaling pathways, which control cytokine production and degranulation. Through an understanding of these mechanisms NPs can be formulated and utilized for numerous applications while mitigating unintended adverse health effects such as allergic immune responses.

Acknowledgments

This was supported by NIEHS grants R01 ES019311 and U19 ES019525 and silver nanomaterials used in this study were procured, characterized and provided by the NIEHS Centers for Nanotechnology Health Implications Research (NCNHIR) Consortium. We would like to acknowledge Susana Hilderbrand for technical assistance; and Hilary Emerson and Brian Powell at Clemson University for access to their ICP-MS. Any opinions, findings, conclusions or recommendations expressed herein are those of the authors and do not necessarily reflect the views of the National Institute of Environmental Health Sciences/NIH.

Abbreviations

AgNPs	Silver Nanoparticles
BLT-2	Blocking Lipid Transporter-2 (Scavenger Receptor B1 inhibitor)
BMMC	Bone marrow-derived mast cells
C110	110 nm spherical silver nanoparticles suspended in citrate
C20	20 nm spherical silver nanoparticles suspended in citrate
Lamp2	Lysosome-associated membrane proteins 2
NPs	Nanoparticles
OPN	Osteopontin
P110	110 nm spherical silver nanoparticles suspended in polyvinylpyrrolidone
P20	20 nm spherical silver nanoparticles suspended in polyvinylpyrrolidone
P550	Nanoplates with optical resonance peak at specific wavelengths of 550 nm suspended in polyvinylpyrrolidone
P850	Nanoplates with optical resonance peak at specific wavelengths of 850 nm suspended in polyvinylpyrrolidone
PVP	Polyvinylpyrrolidone
SR-B1	Scavenger Receptor B1

References

- Baranova IN, Vishnyakova TG, Bocharov AV, Kurlander R, Chen Z, Kimelman ML, Remaley AT, Csako G, Thomas F, Eggerman TL, Patterson AP. Serum amyloid A binding to CLA-1 (CD36 and LIMPII analogous-1) mediates serum amyloid A protein-induced activation of ERK1/2 and p38 mitogen-activated protein kinases. *J Biol Chem.* 2005; 280:8031–8040. [PubMed: 15576377]
- Berezin AE, Kremzer AA. Circulating osteopontin as a marker of early coronary vascular calcification in type two diabetes mellitus patients with known asymptomatic coronary artery disease. *Atherosclerosis.* 2013; 229:475–481. [PubMed: 23880208]
- Brown JM, Swindle EJ, Kushnir-Sukhov NM, Holian A, Metcalfe DD. Silica-directed mast cell activation is enhanced by scavenger receptors. *Am J Respir Cell Mol Biol.* 2007; 36:43–52. [PubMed: 16902192]
- Brown JM, Wilson TM, Metcalfe DD. The mast cell and allergic diseases: role in pathogenesis and implications for therapy. *Clin Exp Allergy.* 2008; 38:4–18. [PubMed: 18031566]
- Canton J, Neculai D, Grinstein S. Scavenger receptors in homeostasis and immunity. *Nat Rev Immunol.* 2013; 13:621–634. [PubMed: 23928573]
- Carlson C, Hussain SM, Schrand AM, Braydich-Stolle KL, Hess KL, Jones RL, Schlager JJ. Unique Cellular Interaction of Silver Nanoparticles: Size-Dependent Generation of Reactive Oxygen Species. *The Journal of Physical Chemistry B.* 2008; 112:13608–13619. [PubMed: 18831567]
- Catanese MT, Loureiro J, Jones CT, Dorner M, von Hahn T, Rice CM. Different requirements for scavenger receptor class B type I in hepatitis C virus cell-free versus cell-to-cell transmission. *J Virol.* 2013; 87:8282–8293. [PubMed: 23698298]
- Champion JA, Katare YK, Mitragotri S. Particle shape: A new design parameter for micro- and nanoscale drug delivery carriers. *Journal of Controlled Release.* 2007; 121:3–9. [PubMed: 17544538]
- Champion JA, Mitragotri S. Role of target geometry in phagocytosis. *Proc Natl Acad Sci U S A.* 2006; 103:4930–4934. [PubMed: 16549762]
- Christensen FM, Johnston HJ, Stone V, Aitken RJ, Hankin S, Peters S, Aschberger K. Nano-silver – feasibility and challenges for human health risk assessment based on open literature. *Nanotoxicology.* 2010; 4:284–295. [PubMed: 20795910]
- Dellinger A, Zhou Z, Norton SK, Lenk R, Conrad D, Kopley CL. Uptake and distribution of fullerenes in human mast cells. *Nanomedicine.* 2010; 6:575–582. [PubMed: 20138243]
- Dong C, Yan Z, Kokx J, Chrisey DB, Dinu CZ. Antibacterial and surface-enhanced Raman scattering (SERS) activities of AgCl cubes synthesized by pulsed laser ablation in liquid. *Applied Surface Science.* 2012; 258:9218–9222.
- Echegoyen Y, Nerín C. Nanoparticle release from nano-silver antimicrobial food containers. *Food and Chemical Toxicology.* 2013; 62:16–22. [PubMed: 23954768]
- Eyre NS, Drummer HE, Beard MR. The SR-BI partner PDZK1 facilitates hepatitis C virus entry. *PLoS Pathog.* 2010; 6:e1001130. [PubMed: 20949066]
- Goldstein JL, Ho YK, Basu SK, Brown MS. Binding site on macrophages that mediates uptake and degradation of acetylated low density lipoprotein, producing massive cholesterol deposition. *Proc Natl Acad Sci U S A.* 1979; 76:333–337. [PubMed: 218198]
- Hamilton RF Jr, Wu Z, Mitra S, Shaw PK, Holian A. Effect of MWCNT size, carboxylation, and purification on in vitro and in vivo toxicity, inflammation and lung pathology. *Part Fibre Toxicol.* 2013; 10:57. [PubMed: 24225053]
- Harris BJ, Dalhaimer P. Particle shape effects in vitro and in vivo. *Front Biosci (Schol Ed).* 2012; 4:1344–1353. [PubMed: 22652876]
- Huang YF, Liu H, Xiong X, Chen Y, Tan W. Nanoparticle-mediated IgE-receptor aggregation and signaling in RBL mast cells. *J Am Chem Soc.* 2009; 131:17328–17334. [PubMed: 19929020]
- Iwaki S, Tkaczyk C, Satterthwaite AB, Halcomb K, Beaven MA, Metcalfe DD, Gilfillan AM. Btk plays a crucial role in the amplification of Fc epsilonRI-mediated mast cell activation by kit. *J Biol Chem.* 2005; 280:40261–40270. [PubMed: 16176929]

- Katwa P, Wang X, Urankar RN, Podila R, Hilderbrand SC, Fick RB, Rao AM, Ke PC, Wingard CJ, Brown JM. A carbon nanotube toxicity paradigm driven by mast cells and the IL-(3)(3)/ST(2) axis. *Small*. 2012; 8:2904–2912. [PubMed: 22777948]
- Kittler S, Greulich C, Diendorf J, Köller M, Epple M. Toxicity of Silver Nanoparticles Increases during Storage Because of Slow Dissolution under Release of Silver Ions. *Chemistry of Materials*. 2010; 22:4548–4554.
- Krieger M, Herz J. Structures and functions of multiligand lipoprotein receptors: macrophage scavenger receptors and LDL receptor-related protein (LRP). *Annu Rev Biochem*. 1994; 63:601–637. [PubMed: 7979249]
- Landschulz KT, Pathak RK, Rigotti A, Krieger M, Hobbs HH. Regulation of scavenger receptor, class B, type I, a high density lipoprotein receptor, in liver and steroidogenic tissues of the rat. *J Clin Invest*. 1996; 98:984–995. [PubMed: 8770871]
- Levard C, Mitra S, Yang T, Jew AD, Badireddy AR, Lowry GV, Brown GE. Effect of Chloride on the Dissolution Rate of Silver Nanoparticles and Toxicity to *E. coli*. *Environmental Science & Technology*. 2013; 47:5738–5745. [PubMed: 23641814]
- Li R, Wang X, Ji Z, Sun B, Zhang H, Chang CH, Lin S, Meng H, Liao YP, Wang M, Li Z, Hwang AA, Song TB, Xu R, Yang Y, Zink JI, Nel AE, Xia T. Surface charge and cellular processing of covalently functionalized multiwall carbon nanotubes determine pulmonary toxicity. *ACS Nano*. 2013; 7:2352–2368. [PubMed: 23414138]
- Marquis BJ, Liu Z, Braun KL, Haynes CL. Investigation of noble metal nanoparticle[small zeta]-potential effects on single-cell exocytosis function in vitro with carbon-fiber microelectrode amperometry. *Analyst*. 2011; 136:3478–3486. [PubMed: 21170444]
- Marquis BJ, Maurer-Jones MA, Braun KL, Haynes CL. Amperometric assessment of functional changes in nanoparticle-exposed immune cells: varying Au nanoparticle exposure time and concentration. *Analyst*. 2009; 134:2293–2300. [PubMed: 19838418]
- Maurer-Jones MA, Lin YS, Haynes CL. Functional assessment of metal oxide nanoparticle toxicity in immune cells. *ACS Nano*. 2010; 4:3363–3373. [PubMed: 20481555]
- McCurdy JD, Olynych TJ, Maher LH, Marshall JS. Cutting edge: distinct Toll-like receptor 2 activators selectively induce different classes of mediator production from human mast cells. *J Immunol*. 2003; 170:1625–1629. [PubMed: 12574323]
- Medic N, Vita F, Abbate R, Soranzo MR, Pacor S, Fabbretti E, Borelli V, Zabucchi G. Mast cell activation by myelin through scavenger receptor. *J Neuroimmunol*. 2008; 200:27–40. [PubMed: 18657868]
- Miethling-Graff R, Rumpker R, Richter M, Verano-Braga T, Kjeldsen F, Brewer J, Hoyland J, Rubahn HG, Erdmann H. Exposure to silver nanoparticles induces size- and dose-dependent oxidative stress and cytotoxicity in human colon carcinoma cells. *Toxicol In Vitro*. 2014; 28:1280–1289. [PubMed: 24997297]
- Mooberry LK, Nair M, Paranjape S, McConathy WJ, Lacko AG. Receptor mediated uptake of paclitaxel from a synthetic high density lipoprotein nanocarrier. *J Drug Target*. 2010; 18:53–58. [PubMed: 19637935]
- Murao K, Terpstra V, Green SR, Kondratenko N, Steinberg D, Quehenberger O. Characterization of CLA-1, a human homologue of rodent scavenger receptor BI, as a receptor for high density lipoprotein and apoptotic thymocytes. *J Biol Chem*. 1997; 272:17551–17557. [PubMed: 9211901]
- Nishanth RP, Jyotsna RG, Schlager JJ, Hussain SM, Reddanna P. Inflammatory responses of RAW 264.7 macrophages upon exposure to nanoparticles: Role of ROS-NF κ B signaling pathway. *Nanotoxicology*. 2011; 5:502–516. [PubMed: 21417802]
- Nocchetti M, Donnadio A, Ambrogi V, Andreani P, Bastianini M, Pietrella D, Latterini L. Ag/AgCl nanoparticle decorated layered double hydroxides: synthesis, characterization and antimicrobial properties. *Journal of Materials Chemistry B*. 2013; 1:2383–2393.
- Pass HI, Carbone M. Current status of screening for malignant pleural mesothelioma. *Semin Thorac Cardiovasc Surg*. 2009; 21:97–104. [PubMed: 19822280]
- Piccinno F, Gottschalk F, Seeger S, Nowack B. Industrial production quantities and uses of ten engineered nanomaterials in Europe and the world. *Journal of Nanoparticle Research*. 2012; 14:1–11. [PubMed: 22448125]

- Podila R, Brown JM. Toxicity of engineered nanomaterials: a physicochemical perspective. *J Biochem Mol Toxicol*. 2013; 27:50–55. [PubMed: 23129019]
- Podila R, Chen R, Ke PC, Brown JM, Rao AM. Effects of surface functional groups on the formation of nanoparticle-protein corona. *Applied Physics Letters*. 2012:101.
- Project, 2014. Project on Emerging Nanotechnologies. Consumer Products Inventory. Retrieved [2014], from <http://www.nanotechproject.org/cpi>
- Rahman MF, Wang J, Patterson TA, Saini UT, Robinson BL, Newport GD, Murdock RC, Schlager JJ, Hussain SM, Ali SF. Expression of genes related to oxidative stress in the mouse brain after exposure to silver-25 nanoparticles. *Toxicology Letters*. 2009; 187:15–21. [PubMed: 19429238]
- Rigotti A, Trigatti B, Babbit J, Penman M, Xu S, Krieger M. Scavenger receptor BI—a cell surface receptor for high density lipoprotein. *Curr Opin Lipidol*. 1997a; 8:181–188. [PubMed: 9211067]
- Rigotti A, Trigatti BL, Penman M, Rayburn H, Herz J, Krieger M. A targeted mutation in the murine gene encoding the high density lipoprotein (HDL) receptor scavenger receptor class B type I reveals its key role in HDL metabolism. *Proc Natl Acad Sci U S A*. 1997b; 94:12610–12615. [PubMed: 9356497]
- Ryan JJ, Bateman HR, Stover A, Gomez G, Norton SK, Zhao W, Schwartz LB, Lenk R, Kepley CL. Fullerene nanomaterials inhibit the allergic response. *J Immunol*. 2007; 179:665–672. [PubMed: 17579089]
- Shannah JH, Brown JM. Engineered nanomaterial exposure and the risk of allergic disease. *Curr Opin Allergy Clin Immunol*. 2014; 14:95–99. [PubMed: 24378479]
- Shannah JH, Kodavanti UP, Brown JM. Manufactured and airborne nanoparticle cardiopulmonary interactions: a review of mechanisms and the possible contribution of mast cells. *Inhal Toxicol*. 2012; 24:320–339. [PubMed: 22486349]
- Sharma G, Valenta DT, Altman Y, Harvey S, Xie H, Mitragotri S, Smith JW. Polymer particle shape independently influences binding and internalization by macrophages. *Journal of Controlled Release*. 2010; 147:408–412. [PubMed: 20691741]
- Singh RP, Ramarao P. Cellular uptake, intracellular trafficking and cytotoxicity of silver nanoparticles. *Toxicol Lett*. 2012; 213:249–259. [PubMed: 22820426]
- Sung JH, Ji JH, Yoon JU, Kim DS, Song MY, Jeong J, Han BS, Han JH, Chung YH, Kim J, Kim TS, Chang HK, Lee EJ, Lee JH, Yu IJ. Lung Function Changes in Sprague-Dawley Rats After Prolonged Inhalation Exposure to Silver Nanoparticles. *Inhalation Toxicology*. 2008; 20:567–574. [PubMed: 18444009]
- Sunshine JC, Perica K, Schneck JP, Green JJ. Particle shape dependence of CD8+ T cell activation by artificial antigen presenting cells. *Biomaterials*. 2014; 35:269–277. [PubMed: 24099710]
- Tang J, Xiong L, Wang S, Wang J, Liu L, Li J, Yuan F, Xi T. Distribution, translocation and accumulation of silver nanoparticles in rats. *J Nanosci Nanotechnol*. 2009; 9:4924–4932. [PubMed: 19928170]
- Tiwari DK, Jin T, Behari J. Dose-dependent in-vivo toxicity assessment of silver nanoparticle in Wistar rats. *Toxicology Mechanisms and Methods*. 2011; 21:13–24. [PubMed: 21080782]
- Umemoto EY, Speck M, Shimoda LM, Kahue K, Sung C, Stokes AJ, Turner H. Single-walled carbon nanotube exposure induces membrane rearrangement and suppression of receptor-mediated signalling pathways in model mast cells. *Toxicol Lett*. 2014; 229:198–209. [PubMed: 24910985]
- Wingard CJ, Walters DM, Cathey BL, Hilderbrand SC, Katwa P, Lin S, Ke PC, Podila R, Rao A, Lust RM, Brown JM. Mast cells contribute to altered vascular reactivity and ischemia-reperfusion injury following cerium oxide nanoparticle instillation. *Nanotoxicology*. 2011; 5:531–545. [PubMed: 21043986]
- Xia T, Hamilton RF, Bonner JC, Crandall ED, Elder A, Fazlollahi F, Girtsman TA, Kim K, Mitra S, Ntim SA, Orr G, Tagmount M, Taylor AJ, Telesca D, Tolic A, Vulpe CD, Walker AJ, Wang X, Witzmann FA, Wu N, Xie Y, Zink JI, Nel A, Holian A. Interlaboratory evaluation of in vitro cytotoxicity and inflammatory responses to engineered nanomaterials: the NIEHS Nano GO Consortium. *Environ Health Perspect*. 2013; 121:683–690. [PubMed: 23649538]
- Yamaki K, Yoshino S. Comparison of inhibitory activities of zinc oxide ultrafine and fine particulates on IgE-induced mast cell activation. *Biometals*. 2009; 22:1031–1040. [PubMed: 19609684]

- Yang GH, Fan J, Xu Y, Qiu SJ, Yang XR, Shi GM, Wu B, Dai Z, Liu YK, Tang ZY, Zhou J. Osteopontin combined with CD44, a novel prognostic biomarker for patients with hepatocellular carcinoma undergoing curative resection. *Oncologist*. 2008; 13:1155–1165. [PubMed: 18997126]
- Yang W, Lee S, Lee J, Bae Y, Kim D. Silver nanoparticle-induced degranulation observed with quantitative phase microscopy. *J Biomed Opt*. 2010; 15:045005. [PubMed: 20799800]
- Zhu P, Liu X, Trembl LS, Cancro MP, Freedman BD. Mechanism and regulatory function of CpG signaling via scavenger receptor B1 in primary B cells. *J Biol Chem*. 2009; 284:22878–22887. [PubMed: 19542230]

Highlights

- Silver nanoparticles induced mast cell degranulation
- Degranulation was dependent on nanoparticle size, shape and surface coating
- Scavenger receptor B1 is involved in the degranulation of mast cells
- Ag⁺ dissolution did not contribute to mast cell degranulation
- Silver nanoparticles may initiate or promote allergic immune responses

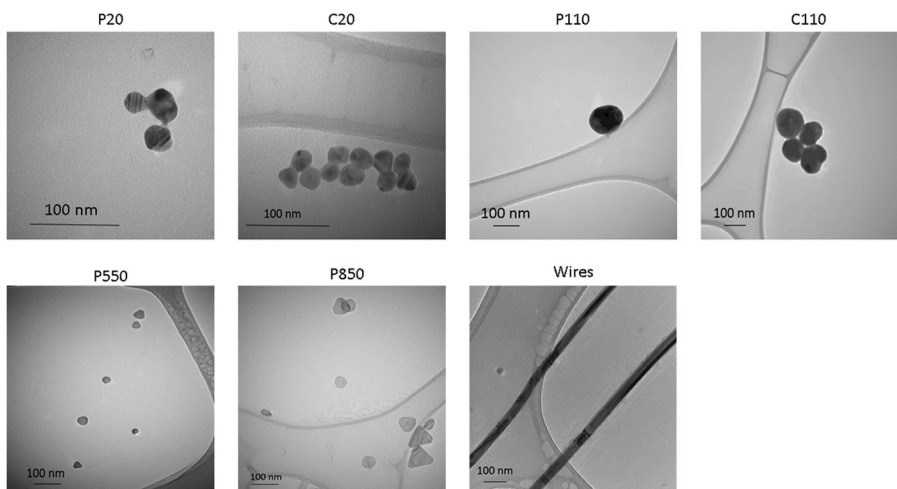


Figure 1.

Representative TEM images demonstrating AgNP shape and size. AgNPs of differing size and shape were evaluated including spherical 20 nm AgNPs suspended in either polyvinylpyrrolidone (P20) or citrate (C20), spherical 110 nm AgNPs suspended in either polyvinylpyrrolidone (P110) or citrate (C110), Ag plates suspended in polyvinylpyrrolidone of either 550 nm resonance (P550) or 850 nm resonance (P850), and Ag nanowires that were suspended in polyvinylpyrrolidone (Wires).

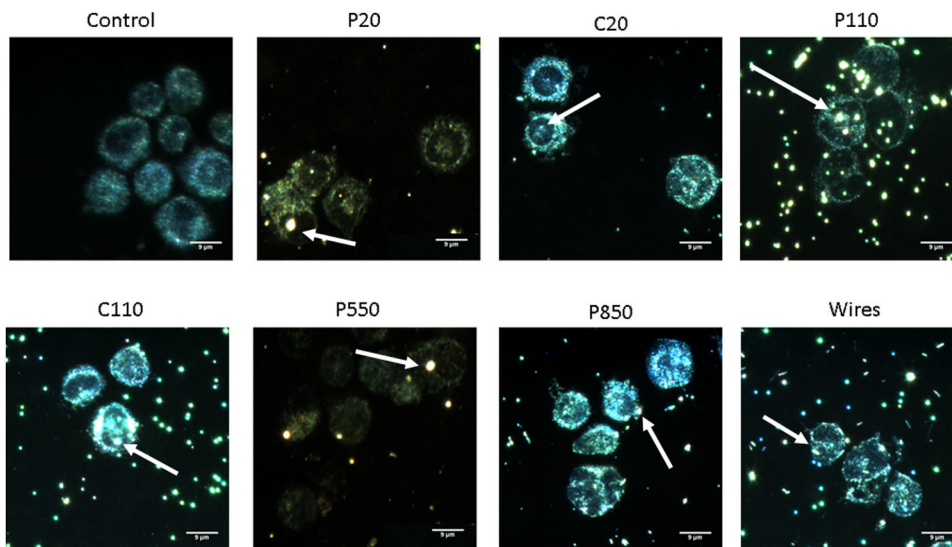


Figure 2. Representative enhanced dark field images of control or AgNP treated bone marrow-derived mast cells (BMMCs). AgNPs of differing sizes and shapes were evaluated including spherical 20 nm AgNPs suspended in either polyvinylpyrrolidone (P20) or citrate (C20), spherical 110 nm AgNPs suspended in either polyvinylpyrrolidone (P110) or citrate (C110), Ag plates suspended in polyvinylpyrrolidone of either 550 nm resonance (P550) or 850 nm resonance (P850), and Ag nanowires that were suspended in polyvinylpyrrolidone (Wires).

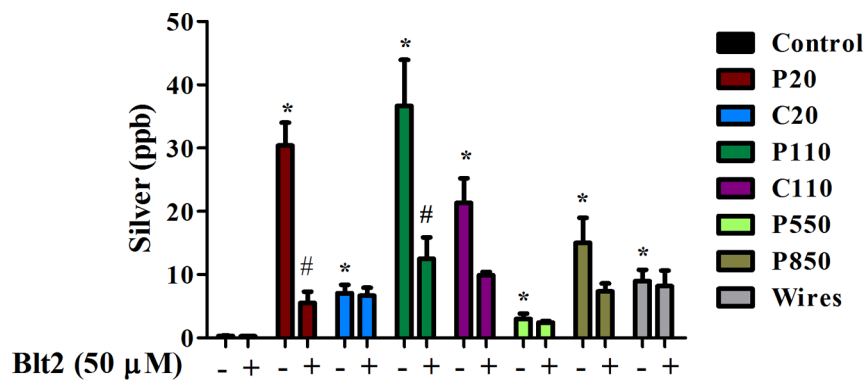
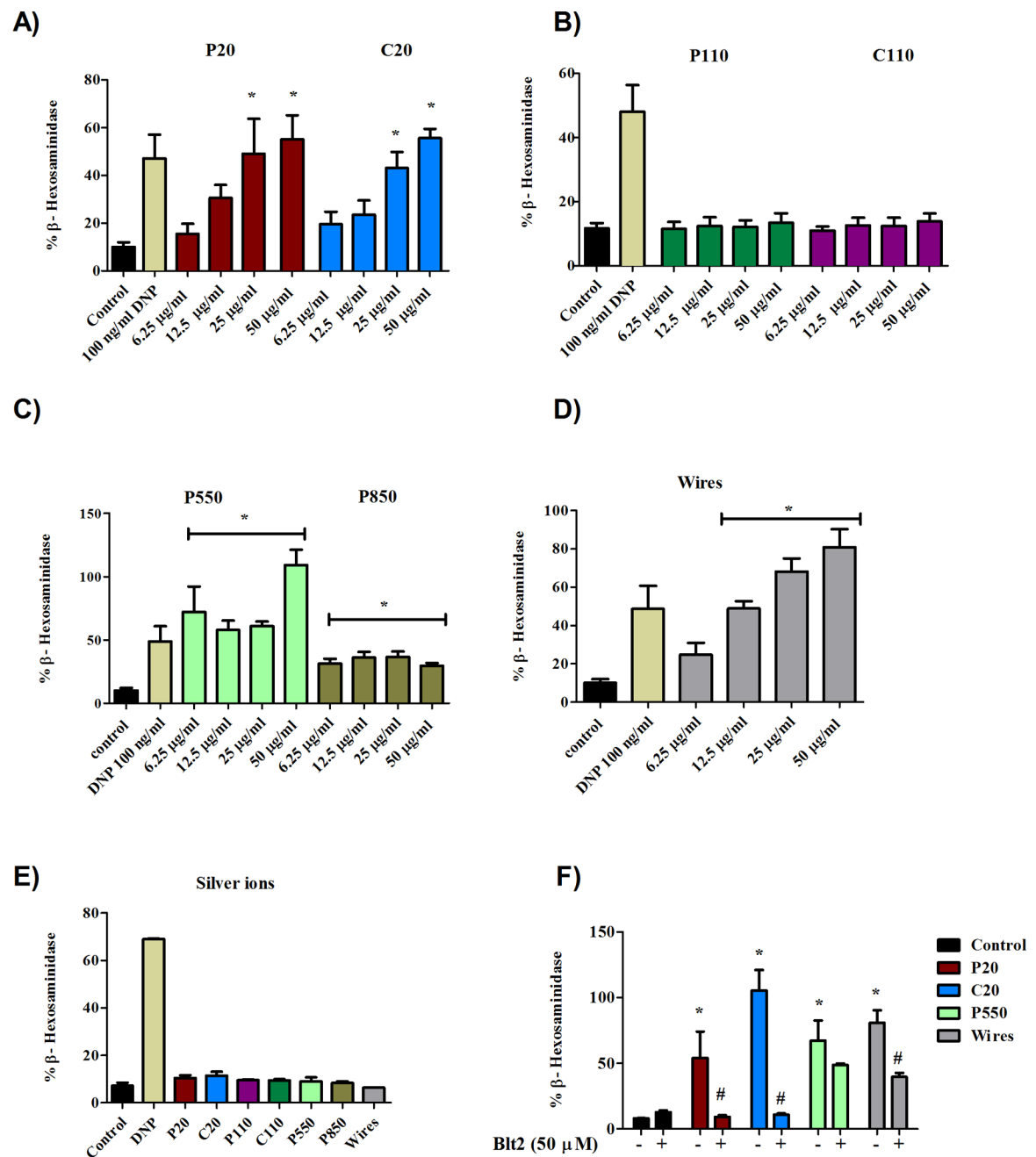


Figure 3. ICP-MS measurement of AgNP uptake by bone marrow-derived mast cells (BMMCs). Cells were pretreated with or without the scavenger receptor B1 (SR-B1) inhibitor Blt2 prior to AgNP exposure. Values are expressed as mean \pm SEM (n=3/group). * Indicates significant difference from control group ($p < 0.05$). # Indicates significant difference of Blt2 pretreated group compared to Blt2 untreated group ($p < 0.05$).

**Figure 4.**

Mast cell degranulation was evaluated by measuring release of β -hexosaminidase into the supernatant 1 h following AgNP exposure. A) Bone marrow derived mast cell (BMMC) degranulation following exposure to spherical polyvinylpyrrolidone (PVP) coated (red) or citrate coated 20 nm (blue) AgNPs. B) BMMC degranulation following exposure to spherical PVP coated (green) or citrate coated 110 nm (purple) AgNPs. C) 550 nm or 850 nm resonant AgNP plates. D) BMMC degranulation following exposure to PVP coated Ag nanowires. E) BMMC degranulation following exposure to Ag^+ ions. F) BMMC degranulation of samples pretreated with or without the scavenger receptor B1 (SR-B1)

inhibitor Blt2. Values are expressed as mean \pm SEM (n=3/group). * Indicates significant difference from controlled group (p \leq 0.05). # Indicates significant difference of Blt2 pretreated group compared to Blt2 untreated group (p \leq 0.05).

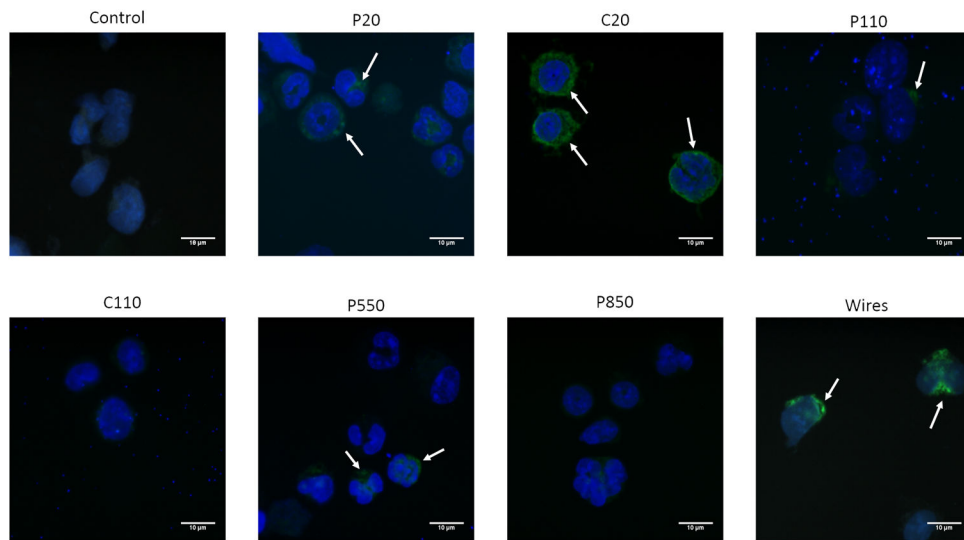


Figure 5.

Lysosome-associated membrane protein 2 (Lamp2) expression (green) in bone marrow derived mast cells (BMMCs) following AgNP exposure. BMMCs were collected 1 h following AgNP exposure, washed, spun onto glass slides and immunofluorescently stained with DAPI to identify the nucleus (blue) and Lamp2 to determine BMMC degranulation (green).

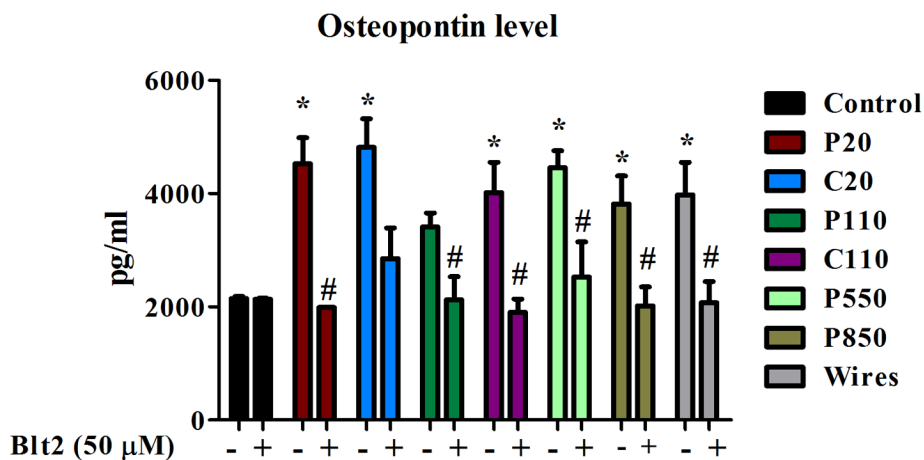


Figure 6. Osteopontin (OPN) levels were measured in supernatants by ELISA. BMMCs were pretreated with or without the scavenger receptor B1 inhibitor Blt2 before AgNPs exposure. Values are expressed as mean \pm SEM (n=3/group). * Indicates significant difference from controlled group (p < 0.05). # Indicates significant difference of Blt2 pretreated group compared to Blt2 untreated group (p < 0.05).

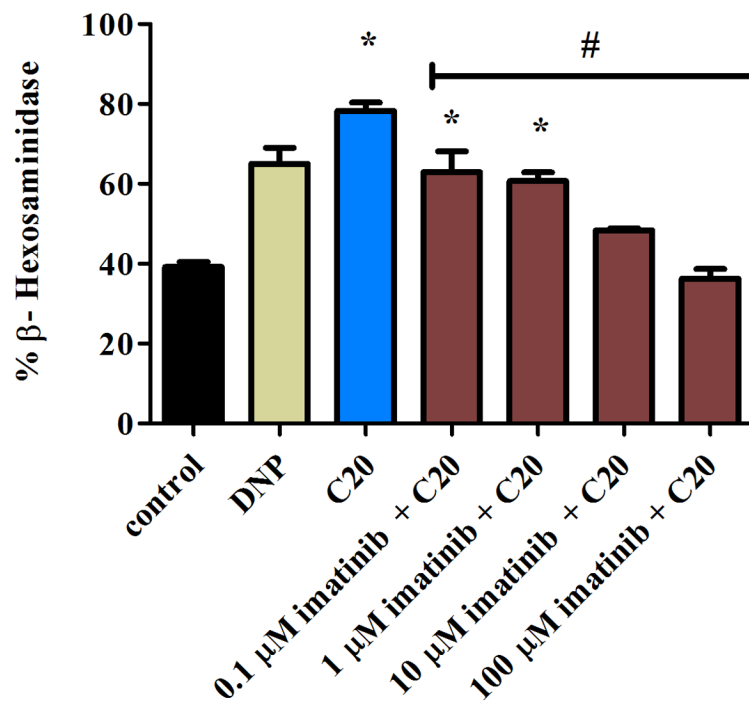


Figure 7. Bone marrow-derived mast cell (BMMC) degranulation was evaluated by measuring release of β -hexosaminidase 1 h following exposure to 50 μ g/ml of 20 nm citrate coated AgNPs. Cells were pretreated with or without imatinib for 30 min at concentration of 0.1, 1, 10, 100 μ M. * Indicates significant difference from controlled group ($p < 0.05$). # Indicates significant difference of BIt2 pretreated group compared to BIt2 untreated group ($p < 0.05$).

Table 1

Characterization of AgNPs. Hydrodynamic size and zeta potential were determined by ZetaSizer Nano and TEM.

	P20	C20	P110	C110	P550	P850	Wires
Hydrodynamic Size (nm) (n=3/group)	28.75 ± 1.95	26.61 ± 4.09	111.5 ± 0.17	132.85 ± 2.05	37.54 ± 0.28	71.49 ± 2.59	315.75 ± 2.33
TEM	21 ± 3	18.5 ± 5	112 ± 2	109 ± 3	42 ± 5	Base: 75 ± 5 Height: 105 ± 10	Length: 1250 ± 100 Diameter: 105 ± 10
Zeta Potential (mV)	-39.9	-49.7	-27.3	-54.9	-29.6	-32.5	-25.9